Comparison of Optic Nerve Head Microvasculature Between Normal-Tension Glaucoma and Nonarteritic Anterior Ischemic Optic Neuropathy

Ji-Ah Kim,[1] Eun Ji Lee,[2] Tae-Woo Kim,[2] Hee Kyung Yang,[2] and Jeong-Min Hwang[2]

[1]Department of Ophthalmology, Ewha Womans University College of Medicine, Ewha Womans University Seoul Hospital, Seoul, Korea
[2]Department of Ophthalmology, Seoul National University College of Medicine, Seoul National University Bundang Hospital, Seongnam, Korea

Correspondence: Eun Ji Lee, Department of Ophthalmology, Seoul National University Bundang Hospital, Seoul National University College of Medicine, 82, Gumi-ro, 173 Beon-gil, Bundang-gu, Seongnam, Gyeonggi-do 463-707, Korea;
opticdisc@gmail.com.

Received: April 11, 2021
Accepted: July 19, 2021
Published: August 16, 2021

Citation: Kim JA, Lee EJ, Kim TW, Yang HK, Hwang JM. Comparison of optic nerve head microvasculature between normal-tension glaucoma and nonarteritic anterior ischemic optic neuropathy. *Invest Ophthalmol Vis Sci.* 2021;62(10):15.
https://doi.org/10.1167/iovs.62.10.15

Purpose. To compare the microvasculature of the optic nerve head (ONH) and peripapillary tissues in eyes with normal-tension glaucoma (NTG) and nonarteritic anterior ischemic optic neuropathy (NAION) using optical coherence tomography angiography (OCTA).

Methods. Thirty-eight eyes with treatment-naïve NTG, 38 eyes with NAION matched for retinal nerve fiber layer (RNFL) thickness in each superior and inferior quadrant, and 38 healthy eyes matched by age were included. ONH and peripapillary retinal microvasculature was evaluated in en face images obtained using OCTA. Vessel density (VD) was calculated as the percent area occupied by vessels in the measured region in each layer segmented into the prelaminar tissue (PLT), lamina cribrosa (LC), and peripapillary retina (PR).

Results. VDs in the PLT and LC were lower in NTG eyes than in both NAION and healthy eyes ($P \leq 0.008$), and did not differ between the NAION and healthy eyes. VDs in the PR did not differ between the NTG and NAION eyes. In intersectoral comparisons, VDs in the PLT ($P = 0.030$) and LC ($P = 0.028$) were lower in the affected than in the unaffected sector of eyes with NTG, but the differences did not occur in eyes with NAION. VD in the PR was lower in the affected than in the unaffected sector in both NTG and NAION eyes (both $P < 0.001$).

Conclusions. Despite similar degrees of RNFL loss and VD decreases in the PR, VDs in the ONH differed between eyes with NTG and NAION, indicating different mechanisms of vascular impairment and ONH damage in each condition.

Keywords: glaucoma, NAION, OCT angiography, optic nerve head

Glaucoma and nonarteritic anterior ischemic optic neuropathy (NAION) are the most common causes of irreversible optic neuropathy in adults. Although characteristics of the acute phase of NAION are diagnostic for this condition, NAION may present with enlargement of the optic cup in the nonacute phase, simulating glaucomatous optic nerve head (ONH) cupping. Both glaucoma and NAION involve thinning of the retinal nerve fiber layer (RNFL) and resulting visual field defects.[1,2] Moreover, the patterns of RNFL loss and visual field defects may be similar in these conditions,[2,3] making it challenging to distinguish between them diagnostically. However, their disease processes and prognoses differ, and treatment approaches should be differentiated to halt further progressive damage in glaucoma, emphasizing the importance of an accurate differential diagnosis of these diseases.

Although the pathophysiological processes underlying glaucoma and NAION may differ, impaired perfusion in the ONH is suggested as a potential pathogenic factor in both. NAION is thought to result from a circulatory insufficiency within the retrolaminar portion of the ONH, which is supplied by the short posterior ciliary arteries (SPCA).[4–8] Fluorescein and indocyanine studies in NAION have shown delayed optic disc filling in the prelaminar tissue (PLT), with normal choroidal circulation, suggesting that the vasculopathy is located in the paraoptic branches of the SPCA, after their branching from the choroidal branches, rather than in the SPCA itself.[9,10] On the other hand, SPCA supplies the anterior ONH tissues including the PLT and lamina cribrosa (LC), the key structure involved in glaucomatous optic neuropathy. Thus, SPCA circulation has also been of particular interest in understanding the vascular pathogenesis of glaucoma, with studies showing that glaucoma is associated with compromised ocular blood flow[11] or decreased ONH perfusion.[12–18] However, impaired perfusion is not considered as a potent factor as mechanical stress in eyes with glaucomatous optic neuropathy.

Our group showed that vessel density (VD) in the ONH, as evaluated by optical coherence tomography (OCT) angiography (OCTA), was lower in patients with normal-

tension glaucoma (NTG) than in normal controls.[19] Intriguingly, the decreased VD in the LC was associated with the degree of LC deformation, which is considered an indicator of the amount of mechanical stress.[20–22] These findings suggested that mechanical stress may be affect the microvasculature within the ONH, possibly by compression of capillaries within the LC.

Although the LC was found to be less deformed in NAION than in NTG eyes with a similar degree of RNFL loss,[23] little is known regarding the microvasculature within the ONH of eyes with NAION. Because the mechanisms of ONH damage differ in eyes with NTG and NAION, we hypothesized that the microvasculature in the ONH may also differ in these two diseases. This study therefore examined the ONH and peripapillary microvasculature in RNFL thickness-matched eyes with NTG and NAION, in comparison with the microvasculature of healthy control eyes. The findings of this study may help not only in differentiating between the two diseases, but also in better understanding their pathophysiology.

Methods

Study Subjects

This study involved subjects with NTG and healthy subjects who were enrolled in the Investigating Glaucoma Progression Study, which is an ongoing prospective study at the Glaucoma Clinic of Seoul National University Bundang Hospital. This study also involved subjects with NAION who visited Seoul National University Bundang Hospital from January 2016 to May 2018. The study protocol was approved by the Institutional Review Board of Seoul National University Bundang Hospital and followed the tenets of the Declaration of Helsinki. Written informed consent to participate was obtained from patients with NTG. The charts of patients with NAION were reviewed retrospectively, with informed consent waived by the institutional review board.

Each subject underwent comprehensive ophthalmic examinations, which included assessments of best-corrected visual acuity, Goldmann applanation tonometry, a refraction test, slit-lamp biomicroscopy, gonioscopy, stereo disc photography, red-free fundus photography (Kowa VX-10; Kowa Medicals, Torrance, CA), standard automated perimetry (Humphrey Field Analyzer II 750, 24-2 Swedish interactive threshold algorithm; Carl Zeiss Meditec, Dublin, CA), measurement of circumpapillary RNFL thickness using spectral-domain OCT (Spectralis, Heidelberg Engineering, Heidelberg, Germany), and swept-source OCTA (DRI OCT Triton, Topcon, Tokyo, Japan). Other ophthalmic examinations included measurements of corneal curvature (KR-1800, Topcon), central corneal thickness (Orbscan II, Bausch & Lomb Surgical, Rochester, NY), and axial length (IOLMaster version 5, Carl Zeiss Meditec).

A clinical history was also obtained from each participant, including demographic characteristics and the presence of cold extremities, migraine, and other systemic conditions. Definition of NTG, NAION, and healthy subjects, criteria for inclusion and exclusion, and the measurement of blood pressure and cup-to-disc ratio are described in the Appendix in the Supplement.

Patients in the NTG group were required to be treatment naïve to rule out the potential effects of IOP and IOP-lowering medications on the ONH VD.[24] IOP was measured and OCTA scans of the ONH performed before the initiation of ocular hypotensive treatment. In each patient with NTG and NAION, either the superotemporal or inferotemporal sector of the eye affected by disease (i.e., RNFL defect with corresponding hemi visual field defect) was defined as the affected sector. NAION subjects were matched 1:1 with patients with NTG based on age and RNFL thicknesses in the superior and inferior quadrants. Healthy subjects were matched for age with NAION and NTG groups. If both eyes were eligible for inclusion, one eye was selected randomly for each patient.

OCTA Measurements of VD

Detailed image acquisition using OCTA of the optic disc is described in the Appendix in the Supplement.

The DRI OCT Triton device allows the microvasculature in the layer of interest to be evaluated in a customized manner. Using manual segmentation, en face OCTA images were first produced in the segmented layer of the PLT (from the internal limiting membrane to the anterior LC border), the LC (from its anterior to its posterior border), and the peripapillary retina (PR; from the internal limiting membrane to the retinal pigment epithelium), as described previously (Fig. 1).[19,21] The scanned images were extracted from the OCTA instrument and imported into publicly available ImageJ software (National Institutes of Health, Bethesda, MD; http://imagej.nih.gov/ij/). Because contrast among en face images can differ, resulting in a falsely larger or smaller VD, the extracted en face images were binarized according to Otsu's method.[25] This method assumes that each image contains two classes of pixels, which are distributed bimodally, with the optimum threshold calculated by minimizing intraclass variance and maximizing interclass variance.[26] Each black region was considered a vascular area, with the number of pixels in each black region quantified with ImageJ software.

Regions of interest (ROIs) for PLT and PR were determined based on Bruch's membrane opening (inner ellipse) and a 750-µm-wide elliptical annulus extending outward from the Bruch's membrane opening (outer ellipse). The ROI encompassed by the inner ellipse was used to assess VD in the PLT, whereas the ROI between the inner and outer ellipses was used to assess VD in the PR. The ROI for the LC was determined based on the cup of the disc, in which LC vasculature is clearly visible in OCTA en face images.[19,21] In the en face OCTA, the cup area was clearly distinguishable as an area of high signal, as opposed to the adjacent dark signal of the rim tissue (Fig. 1).

The areas covered by large retinal vessels observed on color disc photography were considered as projection artifacts, and were excluded manually from the ROIs. To do this, the en face OCTA image was superimposed on the color fundus image, which was obtained simultaneously with OCTA imaging, using the IMAGEnet6 software provided by the manufacturer. The major retinal vessels shown in the color disc photographs were considered the sources of vascular shadowing and projection artifact, and manually delineated using ImageJ software (National Institutes of Health; http://imagej.nih.gov/ij/) and removed from the VD analysis (Fig. 1).

The VD in each ROI was calculated by dividing the number of pixels in the vascular area by the total number of pixels in the ROI and was expressed as a percentage. In addition, superior and inferior VDs in each ROI were calculated in the hemisectors divided according to the foveal–disc axis. The foveal–disc axis was determined based on the infrared image obtained using the Spectralis OCT system. The en

Investigative Ophthalmology & Visual Science

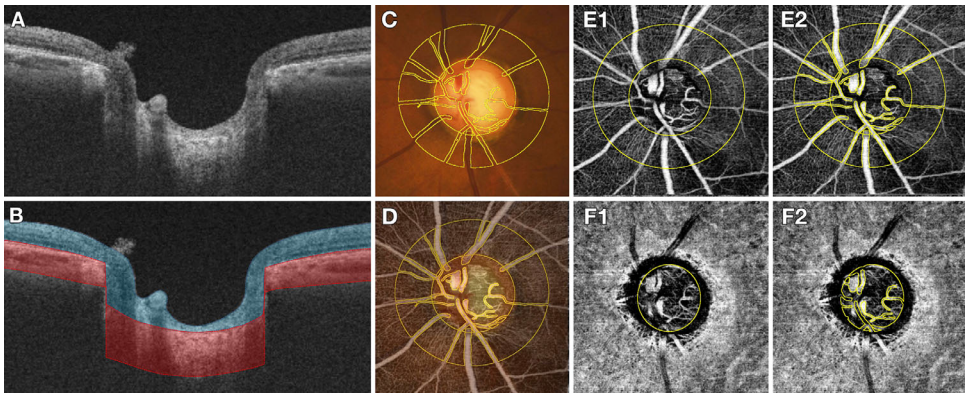

Figure 1. Production of en face OCTA images, segmented into layers, of the PLT, LC, and PR, and determination of ROI. (**A**) B-scan image of an ONH. (**B**) Same image as (**A**), indicating the segmented layers of the PLT and PR (*blue area*) and the LC and peripapillary choroid (*red area*), producing the en face OCTA images in (**E**) and (**F**), respectively. (**C**) Color disc photograph with manually delineated major retinal vessels. (**D**) Superimposed image of color disc photograph and en face OCTA image. (**E**) En face OCTA image at the level of the PLT and PR. The *inner and outer ellipses* indicate the Bruch's membrane opening (BMO) and the 750-µm-wide elliptical annulus extending outward from the BMO, respectively. The ROI encompassed by the *inner ellipse* was used to assess VD in the PLT, and the ROI between the *inner* and *outer ellipses* was used to assess VD in the PR. (**F**) En face OCTA image at the level of the LC. At this level, the cup area is clearly distinguishable as an area of high signal, opposed to the adjacent dark signal of the rim tissue. The ROI was determined based on the optic cup in which the LC vasculature was clearly visible in the en face image, and was used to assess VD in the LC. (**E2**) and (**F2**) are the same images as (**E1**) and (**F1**) indicating large retinal vessels and projection artifacts that were manually excluded from measurements of VD.

face OCTA image was aligned in the same orientation as the infrared image, by superimposing the OCTA image over the infrared image using Photoshop (version 12.0, Adobe Systems, San Jose, CA).

The manual selection of ROI and VD measurements were done by two experienced observers (J.-A.K. and E.J.L.) who were masked to the clinical information of participants. The average of the measurements from each of the two observers was used for analysis.

Data Analysis

Except where stated otherwise, data are presented as mean ± standard deviation. The interobserver agreements for measuring the VDs were assessed by calculation of intraclass correlation coefficients and 95% confidence intervals. Raw data were subjected to Bonferroni correction on the basis of the number of comparisons in each analysis. Comparisons between groups were performed using ANOVA or the Kruskal–Wallis test depending on the assumption of normality using Kolmogorov–Smirnov test with the post hoc Scheffé test or the Mann–Whitney *U* test with Bonferroni correction, respectively, for continuous variables and the χ^2 test for categorical variables. The Wilcoxon paired signed-rank test was performed for intraindividual comparisons. Statistical analyses were performed using the Statistical Package for the Social Sciences software (version 22.0, SPSS, Chicago, IL), with *P* values of less than 0.05 considered statistically significant.

Results

Of the 157 treatment-naïve NTG, 68 NAION, and 186 healthy eyes initially included, 53 eyes (21 NTG, 12 NAION, and 20 healthy eyes) were excluded owing to the presence of a tilted or torted disc, and 57 eyes (29 NTG, 15 NAION, and 13 healthy eyes) were excluded owing to poor visualization of the microvasculature, resulting either from poor image quality or a small ROI. After matching for superior and inferior RNFL thicknesses of NTG and NAION eyes and for age of three groups, each group consisted of 38 eyes (a total of 114 eyes). There was an excellent interobserver agreement in measurements of the VD in the PLT, LC, and PR (intraclass correlation coefficient = 0.957, 0.967, and 0.924 respectively; 95% confidence interval = 0.938–0.970, 0.952–0.977, and 0.889–0.947, respectively).

Table 1 compares the clinical characteristics of NTG, NAION, and healthy subjects. The cup-to-disc ratio was greatest in NTG eyes, followed by healthy and then NAION eyes ($P < 0.001$). Systolic blood pressure ($P = 0.010$), mean arterial pressure ($P = 0.036$), and mean ocular perfusion pressure ($P = 0.013$) were significantly higher in the NAION eyes than in both NTG and healthy eyes.

Twenty eyes in the NAION group showed involvement in a single hemisector, with 17 eyes involving the superior and three eyes involving the inferior hemisector. The remaining 18 NAION eyes showed involvement of both superior and inferior hemisectors. RNFL thicknesses globally and in each hemisector did not differ significantly between the NTG and NAION groups ($P \geq 0.759$, post hoc Scheffé test; data not shown in Table 1).

Global VDs in the PLT and LC were significantly lower in NTG than in both NAION and healthy eyes ($P \leq 0.008$), but were comparable between the NAION and healthy eyes (Table 2, Fig. 2). In contrast, VDs in the PR did not differ between the NTG and NAION eyes ($P = 0.622$, post hoc Scheffé test; data not shown in Table 2).

Sectoral subanalyses were performed in the 20 NTG and 20 NAION eyes with involvement of a single hemisector (Table 2). For healthy subjects, the comparison was made using the corresponding superior or inferior hemisectors to the matched NTG and NAION eyes. VD in the PLT of the affected sector was lower in NTG than in both NAION and healthy eyes ($P = 0.015$), whereas VD in the PLT of the unaffected hemisector did not differ among the three groups ($P = 0.293$). VDs in the LC were lower in both the affected and unaffected sectors of NTG than of both NAION and

Table 1. Clinical Characteristics of NTG, NAION, and Healthy Eyes

Variables	NTG (A) (n = 38)	NAION (B) (n = 38)	Healthy (C) (n = 38)	P Value	Post Hoc§
Age, years	58.1 ± 11.4	61.6 ± 8.8	58.4 ± 9.8	0.256†	
Male, n (%)	24 (63.2)	15 (39.5)	18 (47.4)	0.110*	
Central corneal thickness, µm	540.8 ± 43.2	543.2 ± 22.6	552.7 ± 34.7	0.386†	
Axial length, mm	24.44 ± 1.05	24.12 ± 1.25	24.39 ± 1.27	0.686†	
Spherical equivalent, diopters	−0.94 ± 1.79	−0.52 ± 2.19	−0.63 ± 2.00	0.307‡	
Baseline IOP, mm Hg	12.7 ± 3.0	11.6 ± 3.5	12.7 ± 2.6	0.146‡	
Global RNFL thickness, µm	67.2 ± 14.6	66.7 ± 17.7	96.4 ± 9.5	**<0.001**†	A = B < C
Superior RNFL thickness, µm	70.9 ± 25.1	68.8 ± 27.1	119.2 ± 13.9	**<0.001**†	A = B < C
Inferior RNFL thickness, µm	90.7 ± 29.9	93.1 ± 29.7	124.0 ± 15.5	**<0.001**‡	A = B < C
Visual field mean deviation, dB	−10.31 ± 6.02	−12.70 ± 9.09	−0.25 ± 0.62	**<0.001**†	A = B < C
Optic disc area, mm^2	2.32 ± 0.45	2.38 ± 0.43	2.50 ± 0.38	0.104	
Cup/disc ratio	0.75 ± 0.10	0.32 ± 0.16	0.44 ± 0.09	**<0.001**‡	B < C < A
Systolic BP, mm Hg	123.2 ± 9.6	131.9 ± 12.2	126.0 ± 16.1	**0.010**‡	A = C < B
Diastolic BP, mm Hg	72.4 ± 7.1	76.7 ± 9.1	75.1 ± 10.5	0.096†	
Mean arterial pressure, mm Hg	89.3 ± 6.7	95.1 ± 9.6	92.0 ± 11.6	**0.036**†	A = C < B
Mean ocular perfusion pressure, mm Hg	51.2 ± 5.0	55.7 ± 6.5	52.6 ± 8.0	**0.013**†	A = C < B
Self-reported diabetes, n (%)	7 (18.4)	8 (21.1)	6 (15.8)	0.839*	
Self-reported hypertension, n (%)	13 (34.2)	19 (50.0)	13 (34.2)	0.267*	
Migraine, n (%)	5 (13.2)	4 (10.5)	4 (10.5)	0.917*	
Cold extremities, n (%)	5 (13.2)	0 (0.0)	5 (13.2)	0.065*	

Statistically significant P values in boldface.
BP, blood pressure; IOP, intraocular pressure.
Comparisons were performed using the *χ^2 test, †ANOVA, and ‡Kruskal–Wallis test.
§ Post hoc analysis was performed using the Scheffè test and Mann–Whitney U test with Bonferroni correction.

Table 2. Comparison of VD in the NTG, NAION, and Healthy Eyes

Variables	NTG (A)	NAION (B)	Healthy (C)	P Value	Post Hoc
VD in the PLT, (%)					
Global sector	28.32 ± 6.10	32.70 ± 8.70	31.92 ± 3.50	**0.008**	A < B = C
Affected sector	29.43 ± 5.77	35.94 ± 9.34	32.20 ± 4.47	**0.015**	A < B = C
Unaffected sector	31.30 ± 5.32	34.81 ± 11.27	31.89 ± 3.73	0.293	
VD in the LC, (%)					
Global sector	14.45 ± 5.32	27.39 ± 7.92	30.77 ± 5.69	**<0.001**	A < B = C
Affected sector	14.00 ± 5.21	30.74 ± 9.24	29.57 ± 7.12	**<0.001**	A < B = C
Unaffected sector	17.05 ± 6.37	30.12 ± 8.08	30.89 ± 6.79	**<0.001**	A < B = C
VD in the PR, (%)					
Global sector	27.14 ± 3.83	26.18 ± 4.69	40.15 ± 4.21	**<0.001**	A = B < C
Affected sector	26.73 ± 3.64	26.44 ± 4.36	42.05 ± 4.24	**<0.001**	A = B < C
Unaffected sector	32.12 ± 3.14	32.19 ± 3.81	40.41 ± 3.06	**<0.001**	A = B < C

Values are shown as mean ± standard deviation, with statistically significant P values in boldface. Values that were significant after Bonferroni correction (P < 0.017; 0.05/3) are shown in bold. Statistical significance tested by ANOVA. A post hoc analysis was performed using the Scheffè test.

In comparison of global VD, each group consisted of 38 eyes; in comparison of affected or unaffected sector VD, each group consisted of 20 eyes since eyes with only one hemi-ONH disease were included for the analyses. For healthy subjects, the comparison was made between the sectors matched for the affected and unaffected sectors of NTG and NAION eyes.

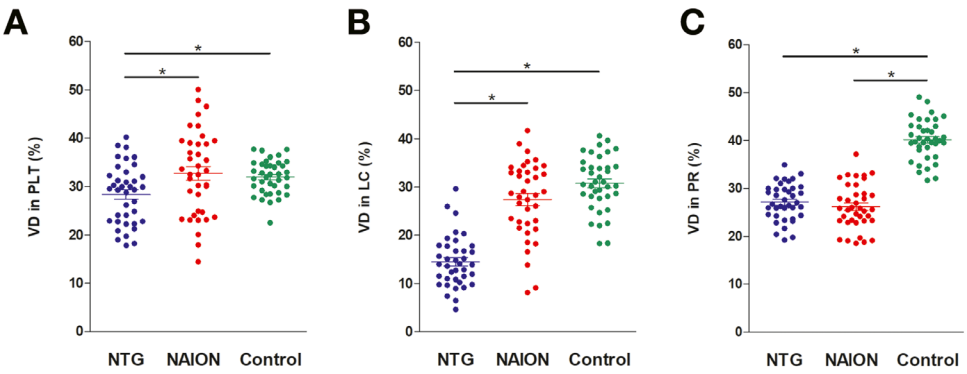

Figure 2. Scatterplots showing VD in PLT (**A**), the LC (**B**), and the PR (**C**) in eyes with NTG, NAION, and healthy controls. VDs in the PLT and LC were significantly lower in eyes with NTG than in both NAION and healthy control eyes. On the other hand, VDs in the PR did not differ significantly between the NTG and NAION eyes, while those were lower in both NTG and NAION eyes than in healthy eyes. The horizontal bars represent the mean ± standard error of the mean. *Asterisks* indicate statistically significant differences (P < 0.05).

Investigative Ophthalmology & Visual Science

Table 3. Comparison of the VD Between Affected and Unaffected Sectors of Single Hemi-ONH Damaged NTG and NAION Eyes

Variables	NTG (n = 20)	NAION (n = 20)
VD in the PLT		
Affected sector (%)	29.43 ± 5.77	35.94 ± 9.34
Unaffected sector (%)	31.30 ± 5.32	34.81 ± 11.27
P value	**0.030**	0.550
VD in the LC		
Affected sector (%)	14.00 ± 5.21	30.74 ± 9.24
Unaffected sector (%)	17.05 ± 6.37	30.12 ± 8.08
P value	**0.028**	0.550
VD in the PR		
Affected sector (%)	26.73 ± 3.64	26.44 ± 4.36
Unaffected sector (%)	32.12 ± 3.14	32.19 ± 3.81
P value	**<0.001**	**<0.001**

Values are shown in mean ± standard deviation, with statistically significant P values in boldface.

Comparisons were performed using the Wilcoxon paired signed rank test.

healthy eyes ($P < 0.001$), although neither differed significantly between the NAION and healthy eyes. VDs in the PR did not differ significantly between the NTG and NAION eyes in either affected or unaffected sectors, with them being significantly lower than those in healthy eyes ($P < 0.001$).

In an intersectoral comparison, VDs in the PLT ($P = 0.030$) and LC ($P = 0.028$) were significantly lower in the affected than in the unaffected sector of eyes with NTG, but the differences did not occur in eyes with NAION (Table 3). The VD in the PR was significantly lower in the affected than in the unaffected sector in both NTG and NAION eyes (both $P < 0.001$).

Figure 3 shows NTG and NAION eyes matched by RNFL thickness in each superior and inferior sector. VDs in the PLT and LC were lower in the NTG than in the NAION eye. In NTG eye, intersectoral difference was also noted for both the VDs in the PLT and LC, with the VDs being lower in the superior affected sector than in the inferior unaffected sector.

Discussion

The present study found that the VD in the PLT and LC was lower in NTG eyes than in RNFL thickness-matched NAION eyes, whereas the VD in the PR did not differ significantly in these two groups. To our knowledge, this study is the first to compare the microvasculature in the ONH and PR between eyes with NTG and NAION.

Although decreased perfusion in the ONH is associated with the pathogenesis of both NTG[15–18] and NAION,[4–8] the mechanisms underlying the relationships between decreased perfusion and disease pathophysiology in these conditions have not yet been determined. The present study showed that the microvasculature in the ONH was lower in NTG than in NAION eyes, and that the decreased ONH microvasculature in NTG was topographically associated with the hemisectoral location of glaucomatous damage. Although the reasons underlying the differences between NTG and NAION in VD in the ONH have not been determined, the difference may be due to differences in ONH morphology between the two diseases.

Posterior deformation of the LC is regarded as a key phenomenon in the pathogenesis of glaucoma.[27–30] LC deformation may not only affect axoplasmic flow at the level of the LC, but also may alter perfusion from the laminar beam capillaries.[31] Recently, our group reported that a larger LC curve (i.e., a greater LC deformation) was associated with a smaller VD in the LC in treatment-naïve NTG eyes.[19] These findings suggest that increased strain in the LC may be associated with decreased perfusion. It has been indeed reported that the LC is more deformed in patients with NTG than in patients with NAION.[23] From this perspective, the lower VD in the LC of the NTG group may be due to a more posteriorly curved LC. On the other hand, LC curvature has been reported to be greater in the hemisphere corresponding to the location of the RNFL defect in NTG eyes.[32] The lower VD in the LC of the affected sector of the NTG group shown in the present study may reflect a more deformed LC at the location of damage.

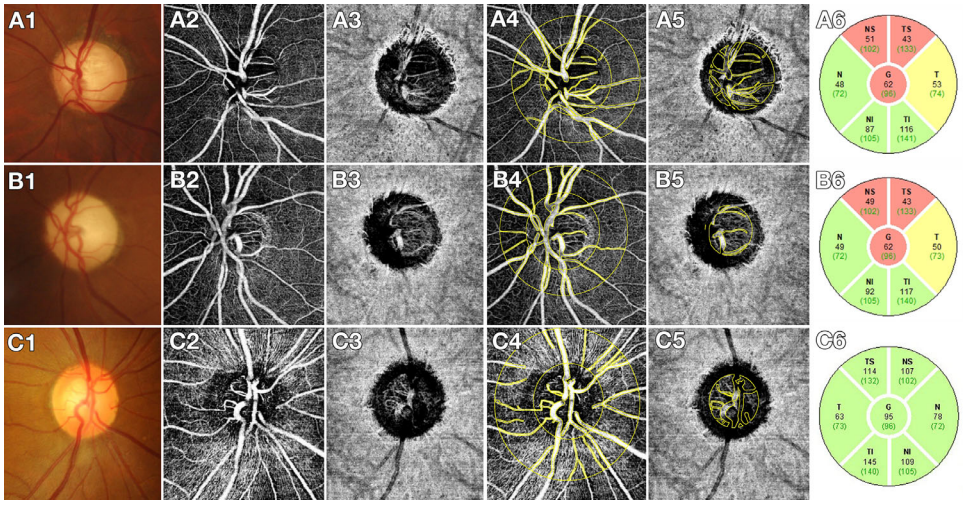

Figure 3. Representative eyes with NTG (**A**) and NAION (**B**), having similar RNFL thickness in each superior and inferior sector, and healthy control eye (**C**). Color disc images (**A1**, **B1**, **C1**), en face OCTA images obtained at segmented layers of the PLT and PR (**A2**, **B2**, **C2**) and the LC and peripapillary choroid (**A3**, **B3**, **C3**). (**A4**, **A5**, **B4**, **B5**, and **C4**, **C5**) Same images as in (**A2**, **A3**), (**B2**, **B3**), and (**C2**, **C3**), respectively, with the ROIs indicated. Note that VD was lower in the PLT (**A2**) and LC (**A3**) in the NTG than in the NAION eyes (**B2**, **B3**), especially in the affected sectors (i.e., superior sector; **A6**, **B6**).

Investigative Ophthalmology & Visual Science

The PLT has been reported to be thicker in NAION than in patients with NTG.[23] This may have been due to the reactive gliosis occurring in NAION eyes,[1,33] as opposed to the thinning of the PLT in NTG, resulting from glaucomatous axonal degeneration. Differences between NTG and NAION in the cup-to-disc ratio and PLT thickness may have resulted in differences in the VD in the PLT between the two groups. The smaller VD in the PLT of the affected sector in the NTG group may represent localized ONH damage, which is characteristic for glaucoma.

The larger VD in the ONH of the NAION group, either the PLT or LC, might also be due to "luxury perfusion",[34,35] which has been described as a vascular response to ischemia characterized by the dilation of blood vessels and increased perfusion in a region surrounding an infarct.[36,37] Acute ischemia of the ONH in eyes with NAION may have induced a vascular autoregulatory response to increased oxygenation in the ischemic portions of the optic disc, resulting in ONH perfusion being maintained in the later stages in NAION. This process may explain the comparable VD in the PLT and LC of NAION and healthy eyes in the present study. NTG, however, is a slowly progressive disease, characterized by primary vascular dysregulation, low diastolic blood pressure, decreased blood flow velocities, smaller retinal vessel diameters, and/or altered endothelial reactivity, suggesting impaired ocular blood flow in patients with NTG. Impaired ocular blood flow likely adds a chronic ischemic insult to the ONH of patients with NTG.[38–42] Decreased perfusion is likely to accompany the chronic course of disease, a mechanism that may explain why ONH VD is lower in NTG than in NAION eyes.

The VD in the PR was previously found to be lower in NTG than in NAION,[43] a finding not consistent with our results.[43] The discrepancy may be attributable to between-group differences in RNFL thickness in the previous study. Although the RNFL thickness did not differ significantly between the two groups in the earlier study,[43] absolute thickness was smaller in NTG than in NAION eyes (69.3 µm *vs.* 78.0 µm). In the present study, eyes with NTG and NAION were matched by RNFL thicknesses in both the affected and unaffected sectors, with the VD in the PR being similar in the two groups (67.2 µm *vs.* 66.7 µm). A recent study reported that VD in the PR was similar in eyes with NAION and those with RNFL thickness-matched primary angle closure glaucoma, which consistent with our finding.[44] Decreased retinal VD was found to correspond topographically to the location of glaucomatous RNFL defects,[45,46] and to correlate with the severity of visual field loss.[47–50] The similar VD in the PR of RNFL thickness-matched patients with NTG and patients with NAION suggests that VD in the PR is indicative of secondary loss or closure of the capillaries in areas of RNFL atrophy, rather than differences in the pathomechanisms of the two diseases.

A decreased VD in the PR, but not in the PLT or LC, indicates that the vascular systems supplying these tissues are independent: the central retinal artery and the SPCA systems, respectively. Recently, Augstburger et al.[51] reported that the rarefaction of the VD in the PR observed on OCTA became more pronounced during progression to the chronic atrophic phase and there was a positive correlation between the VD in the PR and the RNFL thickness in eyes with NAION. Rebolleda et al.[52] also showed that a decrease in the VD in the PR was observed as time goes by and it was correlated with ganglion cell–inner plexiform layer thickness in eyes with NAION. These studies support the notion that PR capillaries may decrease secondary to the progressive loss of the RNFL.

This study had several limitations. First, OCTA measured VD may not be equivalent to anatomic VD. The quantification of the VD relies on speckle noise, so it is vulnerable to shadowing artifact and focus. The morphology of the ONH differs greatly between NAION and NTG eyes, which means that OCTA could have produced biased results owing to the differed morphology. Second, artifacts owing to vascular shadowing or projection onto the underlying tissues are unavoidable with the OCTA modality used in the present study.[53,54] This factor may have limited the analyses of segmented layers, especially of deeper layers. To overcome this limitation, vascular shadowing and projection artifacts were manually excluded from the en face images, and binarized images were used for the evaluation of VD. In addition, attempts have been made to visualize microvessels in the deep ONH, with OCTA able to successfully visualize ONH VD.[19,21,55] Because the manual exclusion of the vascular shadowing and projection artifacts could produce discrepancy between the observers, the selection of ROI and the VD measurements were performed twice from each observer. Third, eyes with a tilted or torted optic disc were excluded. The OCT and OCTA images in the nasal portion of the ONH are influenced by shadowing from the anterior scleral tissue, choroid, and retinal layers in the tilted or torted disc, hampering the accurate evaluation of the VD of deep ONH tissues. The exclusion of such eyes could mean that our results may not be generalizable to all clinical population. Fourth, the present study was also limited by the small sample size of each group, resulting from the incidence of NAION being lower than that of NTG. In addition, some eyes with NAION and small optic disc cups were excluded from the study, because it was difficult to clearly visualize the microvasculature in the LC in these eyes. Fifth, we only included NTG eyes in this study, which is not generalizable to all eyes with glaucoma. However, the IOP has been known to be related to VD in the LC observed on OCTA,[19,21] and thus the bias that could be caused by the influence of IOP should be ruled out by excluding the eyes with a high IOP. Future study is needed including glaucoma group other than NTG.

In conclusion, VD in the ONH was lower in NTG than in RNFL thickness-matched NAION eyes, whereas the VD in the PR did not differ between these two groups. The difference in VD in the ONH likely reflects differences in ONH morphology and in the pathogenesis of the two diseases. Additional studies are needed to determine whether VD differences in ONH tissues can be useful in distinguishing between the two diseases.

Acknowledgments

Supported by Seoul National University Bundang Hospital Research Fund (no. 02-2017-037), Seongnam and by a grant of Patient-Centered Clinical Re search Coordinating Center funded by the Ministry of Health & Welfare, Republic of Korea (Grant no. HI19C0481, HC19C0276).

Disclosure: **J.-A. Kim**, None; **E.J. Lee**, None; **T.-W. Kim**, None; **H.K. Yang**, None; **J.-M. Hwang**, None

References

1. Kaur C, Sivakumar V, Foulds WS. Early response of neurons and glial cells to hypoxia in the retina. *Invest Ophthalmol Vis Sci*. 2006;47(3):1126–1141.

2. Saito H, Tomidokoro A, Sugimoto E, et al. Optic disc topography and peripapillary retinal nerve fiber layer thickness in nonarteritic ischemic optic neuropathy and open-angle glaucoma. *Ophthalmology*. 2006;113(8):1340–1344.
3. Danesh-Meyer HV, Boland MV, Savino PJ, et al. Optic disc morphology in open-angle glaucoma compared with anterior ischemic optic neuropathies. *Invest Ophthalmol Vis Sci*. 2010;51(4):2003–2010.
4. Rootman J, Butler D. Ischaemic optic neuropathy–a combined mechanism. *Br J Ophthalmol*. 1980;64(11):826–831.
5. Lieberman MF, Shahi A, Green WR. Embolic ischemic optic neuropathy. *Am J Ophthalmol*. 1978;86(2):206–210.
6. Quigley HA, Miller NR, Green WR. The pattern of optic nerve fiber loss in anterior ischemic optic neuropathy. *Am J Ophthalmol*. 1985;100(6):769–776.
7. Levin LA, Louhab A. Apoptosis of retinal ganglion cells in anterior ischemic optic neuropathy. *Arch Ophthalmol*. 1996;114(4):488–491.
8. Tesser RA, Niendorf ER, Levin LA. The morphology of an infarct in nonarteritic anterior ischemic optic neuropathy. *Ophthalmology*. 2003;110(10):2031–2035.
9. Arnold AC, Hepler RS. Fluorescein angiography in acute nonarteritic anterior ischemic optic neuropathy. *Am J Ophthalmol*. 1994;117(2):222–230.
10. Oto S, Yilmaz G, Cakmakci S, Aydin P. Indocyanine green and fluorescein angiography in nonarteritic anterior ischemic optic neuropathy. *Retina*. 2002;22(2):187–191.
11. Huber K, Plange N, Remky A, Arend O. Comparison of colour Doppler imaging and retinal scanning laser fluorescein angiography in healthy volunteers and normal pressure glaucoma patients. *Acta Ophthalmol Scand*. 2004;82(4):426–431.
12. Findl O, Rainer G, Dallinger S, et al. Assessment of optic disk blood flow in patients with open-angle glaucoma. *Am J Ophthalmol*. 2000;130(5):589–596.
13. Shiga Y, Omodaka K, Kunikata H, et al. Waveform analysis of ocular blood flow and the early detection of normal tension glaucoma. *Invest Ophthalmol Vis Sci*. 2013;54(12):7699–7706.
14. Shiga Y, Kunikata H, Aizawa N, et al. Optic nerve head blood flow, as measured by laser speckle flowgraphy, is significantly reduced in preperimetric glaucoma. *Curr Eye Res*. 2016;41(11):1447–1453.
15. Schwartz B, Rieser JC, Fishbein SL. Fluorescein angiographic defects of the optic disc in glaucoma. *Arch Ophthalmol*. 1977;95(11):1961–1974.
16. Michelson G, Langhans MJ, Groh MJ. Perfusion of the juxtapapillary retina and the neuroretinal rim area in primary open angle glaucoma. *J Glaucoma*. 1996;5(2):91–98.
17. Piltz-seymour JR, Grunwald JE, Hariprasad SM, Dupont J. Optic nerve blood flow is diminished in eyes of primary open-angle glaucoma suspects. *Am J Ophthalmol*. 2001;132(1):63–69.
18. Hafez AS, Bizzarro RL, Lesk MR. Evaluation of optic nerve head and peripapillary retinal blood flow in glaucoma patients, ocular hypertensives, and normal subjects. *Am J Ophthalmol*. 2003;136(6):1022–1031.
19. Kim JA, Kim TW, Lee EJ, et al. Relationship between lamina cribrosa curvature and the microvasculature in treatment-naive eyes. *Br J Ophthalmol*. 2020;104(3):398–403.
20. Lee SH, Yu DA, Kim TW, et al. Reduction of the lamina cribrosa curvature after trabeculectomy in glaucoma. *Invest Ophthalmol Vis Sci*. 2016;57(11):5006–5014.
21. Kim JA, Kim TW, Lee EJ, et al. Microvascular changes in peripapillary and optic nerve head tissues after trabeculectomy in primary open-angle glaucoma. *Invest Ophthalmol Vis Sci*. 2018;59(11):4614–4621.
22. Lee E, Kim T, Kim H, et al. Comparison between lamina cribrosa depth and curvature as a predictor of progressive retinal nerve fiber layer thinning in primary openaAngle glaucoma. *Ophthalmol Glaucoma*. 2018;1(1):44–51.
23. Lee EJ, Choi YJ, Kim TW, Hwang JM. Comparison of the deep optic nerve head structure between normal-tension glaucoma and nonarteritic anterior ischemic optic neuropathy. *PLoS One*. 2016;11(4):e0150242.
24. Costa VP, Harris A, Stefansson E, et al. The effects of antiglaucoma and systemic medications on ocular blood flow. *Prog Retin Eye Res*. 2003;22(6):769–805.
25. Al-Sheikh M, Ghasemi Falavarjani K, Akil H, Sadda SR. Impact of image quality on OCT angiography based quantitative measurements. *Int J Retina Vitreous*. 2017;3:13.
26. Schneider CA, Rasband WS, Eliceiri KW. NIH Image to ImageJ: 25 years of image analysis. *Nat Methods*. 2012;9(7):671–675.
27. Quigley HA, Addicks EM, Green WR, Maumenee AE. Optic nerve damage in human glaucoma. II. The site of injury and susceptibility to damage. *Arch Ophthalmol*. 1981;99(4):635–649.
28. Bellezza AJ, Rintalan CJ, Thompson HW, et al. Deformation of the lamina cribrosa and anterior scleral canal wall in early experimental glaucoma. *Invest Ophthalmol Vis Sci*. 2003;44(2):623–637.
29. Yang H, Downs JC, Bellezza A, et al. 3-D histomorphometry of the normal and early glaucomatous monkey optic nerve head: prelaminar neural tissues and cupping. *Invest Ophthalmol Vis Sci*. 2007;48(11):5068–5084.
30. Strouthidis NG, Fortune B, Yang H, et al. Longitudinal change detected by spectral domain optical coherence tomography in the optic nerve head and peripapillary retina in experimental glaucoma. *Invest Ophthalmol Vis Sci*. 2011;52(3):1206–1219.
31. Burgoyne CF, Downs JC, Bellezza AJ, et al. The optic nerve head as a biomechanical structure: a new paradigm for understanding the role of IOP-related stress and strain in the pathophysiology of glaucomatous optic nerve head damage. *Prog Retin Eye Res*. 2005;24(1):39–73.
32. Kim JA, Kim TW, Lee EJ, et al. Lamina cribrosa morphology in glaucomatous eyes with hemifield defect in a Korean population. *Ophthalmology*. 2019;126(5):692–701.
33. Jonas JB, Hayreh SS, Tao Y, et al. Optic nerve head change in non-arteritic anterior ischemic optic neuropathy and its influence on visual outcome. *PLoS One*. 2012;7(5):e37499.
34. Yovel OS, Katz M, Leiba H. Magnetic resonance imaging of luxury perfusion of the optic nerve head in anterior ischemic optic neuropathy. *J Neuroophthalmol*. 2012;32(3):256–258.
35. Smith JL. Pseudohemangioma of the optic disc following ischemic optic neuropathy. *J Clin Neuroophthalmol*. 1985;5(2):81–89.
36. Lassen NA. The luxury perfusion syndrome. *Scand J Clin Lab Invest Suppl*. 1968;102:X–A.
37. Friedland S, Winterkorn JM, Burde RM. Luxury perfusion following anterior ischemic optic neuropathy. *J Neuroophthalmol*. 1996;16(3):163–171.
38. Shields MB. Normal-tension glaucoma: is it different from primary open-angle glaucoma? *Curr Opin Ophthalmol*. 2008;19(2):85–88.
39. Park SC, Lee DH, Lee HJ, Kee C. Risk factors for normal-tension glaucoma among subgroups of patients. *Arch Ophthalmol*. 2009;127(10):1275–1283.
40. Mastropasqua R, Fasanella V, Agnifili L, et al. Advance in the pathogenesis and treatment of normal-tension glaucoma. *Prog Brain Res*. 2015;221:213–232.

Investigative Ophthalmology & Visual Science

41. Flammer J, Orgul S, Costa VP, et al. The impact of ocular blood flow in glaucoma. *Prog Retin Eye Res*. 2002;21(4):359–393.
42. Sato EA, Ohtake Y, Shinoda K, et al. Decreased blood flow at neuroretinal rim of optic nerve head corresponds with visual field deficit in eyes with normal tension glaucoma. *Graefes Arch Clin Exp Ophthalmol*. 2006;244(7):795–801.
43. Mastropasqua R, Agnifili L, Borrelli E, et al. Optical coherence tomography angiography of the peripapillary retina in normal-tension glaucoma and chronic nonarteritic anterior ischemic optic neuropathy. *Curr Eye Res*. 2018;43(6):778–784.
44. Fard MA, Suwan Y, Moghimi S, et al. Pattern of peripapillary capillary density loss in ischemic optic neuropathy compared to that in primary open-angle glaucoma. *PLoS One*. 2018;13(1):e0189237.
45. Lee EJ, Lee KM, Lee SH, Kim TW. OCT angiography of the peripapillary retina in primary open-angle glaucoma. *Invest Ophthalmol Vis Sci*. 2016;57(14):6265–6270.
46. Kim SB, Lee EJ, Han JC, Kee C. Comparison of peripapillary vessel density between preperimetric and perimetric glaucoma evaluated by OCT-angiography. *PLoS One*. 2017;12(8):e0184297.
47. Kim GN, Lee E, Kim H, Kim TW. Dynamic range of the peripapillary retinal vessel density for detecting glaucomatous visual field damage. *Ophthalmol Glaucoma*. 2019;2(2):103–110.
48. Rao HL, Pradhan ZS, Weinreb RN, et al. Regional comparisons of optical coherence tomography angiography vessel density in primary open-angle glaucoma. *Am J Ophthalmol*. 2016;171:75–83.
49. Shin JW, Lee J, Kwon J, et al. Regional vascular density-visual field sensitivity relationship in glaucoma according to disease severity. *Br J Ophthalmol*. 2017;101(12):1666–1672.
50. Kumar RS, Anegondi N, Chandapura RS, et al. Discriminant function of optical coherence tomography angiography to determine disease severity in glaucoma. *Invest Ophthalmol Vis Sci*. 2016;57(14):6079–6088.
51. Augstburger E, Zeboulon P, Keilani C, et al. Retinal and choroidal microvasculature in nonarteritic anterior ischemic optic neuropathy: an optical coherence tomography angiography study. *Invest Ophthalmol Vis Sci*. 2018;59(2):870–877.
52. Rebolleda G, Diez-Alvarez L, Garcia Marin Y, et al. Reduction of peripapillary vessel density by optical coherence tomography angiography from the acute to the atrophic stage in non-arteritic anterior ischaemic optic neuropathy. *Ophthalmologica*. 2018;240(4):191–199.
53. Spaide RF, Fujimoto JG, Waheed NK. Image artifacts in optical coherence tomography angiography. *Retina*. 2015;35(11):2163–2180.
54. Akagi T, Iida Y, Nakanishi H, et al. Microvascular density in glaucomatous eyes with hemifield visual field defects: an optical coherence tomography angiography study. *Am J Ophthalmol*. 2016;168:237–249.
55. Numa S, Akagi T, Uji A, et al. Visualization of the lamina cribrosa microvasculature in normal and glaucomatous eyes: a swept-source optical coherence tomography angiography study. *J Glaucoma*. 2018;27(11):1032–1035.